

**Merged-beam measurements of electron-impact excitation of  $\text{Al}^{2+}$  ( $3s^2S \rightarrow 3p^2P$ )**

M. E. Bannister\* and H. F. Krause

*Physics Division, Oak Ridge National Laboratory, Oak Ridge, Tennessee 37831-6372*

N. Djurić, D. B. Popović, and G. H. Dunn

*JILA, University of Colorado and National Institute of Standards and Technology, Boulder, Colorado 80309-0440*

Y.-S. Chung

*Department of Physics, Chungnam National University, 305-764 Daejeon, Korea*

A. C. H. Smith

*Department of Physics and Astronomy, University College London, London WC1E 6BT, United Kingdom*

(Received 19 April 2002; published 18 September 2002)

Absolute cross sections for electron-impact excitation of the  $3s^2S \rightarrow 3p^2P$  transition in  $\text{Al}^{2+}$  were measured near threshold using the merged electron-ion beams energy-loss technique. Although the present results are lower than the previous crossed-beams fluorescence measurements of Dunn *et al.* [Phys. Rev. A **66**, 032706 (2002)] by about 30%, these two experimental excitation cross sections at threshold are in agreement when the energy resolutions and total expanded uncertainties are considered. The present results are in excellent agreement with the published close-coupling calculations, but lie about 30% lower than the distorted-wave predictions.

DOI: 10.1103/PhysRevA.66.032707

PACS number(s): 34.80.Kw

**I. INTRODUCTION**

Collision processes involving electrons and positive ions are ubiquitous in plasma environments. Detailed knowledge of such interactions are crucial to understanding plasmas, both with diagnostic measurements and numerical modeling. While theoretical efforts produce much of the required collision data, careful experimental verification of these predictions is essential. Of particular interest are interactions of electrons with Na-like ions because their line emissions are commonly used as spectroscopic diagnostics of plasma parameters such as electron temperature [1,2]. Electron-impact excitation cross sections have been previously measured for some Na-like ions ( $\text{Mg}^+$ ,  $\text{Si}^{3+}$ ,  $\text{Cl}^{6+}$ ,  $\text{Ar}^{7+}$ ) in the third row of the periodic table [3–6]. In this paper, absolute excitation cross sections are reported for the first allowed transition in  $\text{Al}^{2+}$ . These ions are found in fusion [7] and astrophysical [8] plasmas.

Using a crossed-beam fluorescence technique, Dunn *et al.* [9] measured absolute cross sections for production of 186.3 nm and 185.5 nm photons from the  $\text{Al}^{2+}$  ( $3p^2P \rightarrow 3s^2S$ ) transition from below threshold to about 400 eV. After allowing for cascade from states higher than  $3p^2P$ , their results agree with the unitarized distorted-wave (UDW) calculations of Merts *et al.* [10]. More recent close-coupling (CCV9) predictions of Mitroy and Norcross [11], using a nine-state expansion with pseudostates, lie approximately 30% lower than those measurements. The present experiment seeks to provide further insight into this situation through measurement of absolute cross sections in the near-threshold region using a merged electron-ion beams energy-loss (MEIBEL) tech-

nique [4]. This technique has a higher detection efficiency and narrower energy distribution than the crossed-beams fluorescence technique employed by Dunn *et al.* [9], although the energy range is limited to the near-threshold region. In the energy range covered by the present experiment there is no contribution from cascading from higher states to the fluorescence cross section measured in the earlier experiment, so the fluorescence cross section is simply the excitation cross section and a direct comparison of the two experimental cross sections and the theoretical excitation cross sections are valid.

**II. EXPERIMENT****A. Apparatus**

Details of the apparatus and experimental method have been published previously [12], so only an overview will be presented here. A schematic diagram of the JILA/ORN MEIBEL apparatus is shown in Fig. 1. Ions are extracted at a fixed potential of 17 kV from the ORNL Caprice electron-cyclotron-resonance ion source [13] and magnetically mass-to-charge analyzed. The ion source gases consisted of aluminum vapor produced from Al wire (99.99% purity) in a minioven [14] and nitrogen buffer gas. Electrons produced by a gun featuring a dispenser-type cathode are merged with the  $\text{Al}^{2+}$  ions using a trochoidal analyzer. This “merger” employs crossed **E** and **B** fields to displace the electron beam by about 64 mm perpendicular to both fields. The electrons undergo two gyrations in the **B** field while traversing the merger, ensuring that the electron-beam velocity remains parallel to that of the ion beam. After traversing an electric-field-free merge path (68.5 mm long) in the uniform solenoidal magnetic field ( $\sim 2.5$  mT), the electrons are separated from the ions by a second trochoidal analyzer. This “de-

\*Electronic address: bannisterme@ornl.gov

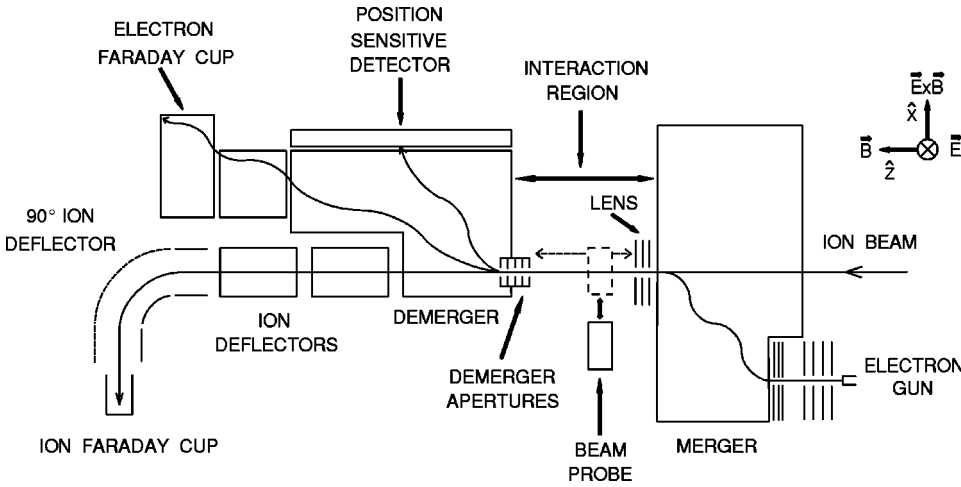


FIG. 1. Schematic of the JILA/ORNL MEIBEL apparatus. See text for details.

merger” deflects electrons that are inelastically scattered from ions onto a position sensitive detector (PSD) consisting of a pair of microchannel plates (MCP) and a resistive anode. The primary (unscattered) electrons are deflected through a smaller angle where they are collected in a Faraday cup. The ions pass through the demerger with negligible deflection and are collected in another Faraday cup after being bent through 90°. Electrons elastically scattered through large angles could also reach the PSD since their forward velocities are close to those of inelastically scattered electrons. However, this is prevented by a series of five apertures (6.5 mm diameter) located at the entrance of the demerger, because these elastically scattered electrons have much larger cyclotron radii in the  $B$  field than the inelastically scattered ones with the same forward velocity.

In addition to the signal from the inelastic-scattering events, large background count rates from electron and ion scattering on residual gas and surfaces are present on the PSD. In order to extract the signal from these backgrounds, both beams are chopped in a phased four-way pattern [12] and counts from the detector are accumulated in four histogramming memories, preserving the position information. The detector counts in the four two-dimensional histograms are individually corrected for the dead times of the position computer, the histogram interface, and the microchannel plates. The inelastic signal as a function of position on the PSD is then obtained from appropriate addition and subtraction of the corrected counts in the four histograms.

### B. Cross-section determination

The excitation cross section  $\sigma$  at an interaction energy in the center-of-mass (c.m.) system,  $E_{c.m.}$ , is determined from

$$\sigma(E_{c.m.}) = \frac{R}{\varepsilon} \left| \frac{v_e v_i}{v_e - v_i} \right| \frac{q e^2}{I_e I_i} F, \quad (1)$$

where  $R$  is the signal count rate of the inelastically scattered electrons,  $\varepsilon$  is the measured PSD detection efficiency ( $0.55 \pm 0.02$ ), and  $v_e$ ,  $v_i$ ,  $I_e$ , and  $I_i$  are the laboratory velocities and currents of the electrons and ions of charge magnitudes  $e$  and  $q e$ , respectively. The form factor  $F$  is given by

$$F = \frac{\int G(x,y,z) dx dy \int H(x,y,z) dx dy}{\int G(x,y,z) H(x,y,z) dx dy dz}. \quad (2)$$

The densities of the two beams,  $G(x,y,z)$  and  $H(x,y,z)$ , are measured with a movable video probe [15] at several positions along the interaction region. The probe consists of a microchannel plate backed by a phosphor-coated coherent fiber-optic bundle to convert the incident particles into an optical signal that is then digitized by a charge-injection device (CID) camera chip [16]. The video signals from the CID camera are then recorded by a frame grabber card and stored on the probe control computer to facilitate the numerical integration of Eq. (2). A grounded grid (50% transmission) in front of the probe allows the electrons to be accelerated through an additional 75 V before striking the MCP.

The data taking protocol consisted of first tuning the electron and ion beams to obtain minimum backgrounds. A simultaneous effort was made to obtain a reasonably good overlap in the interaction region, but with no overlap within and after the demerger apertures in order to prevent elastically scattered electrons from reaching the PSD. This was accomplished by producing a well-collimated electron beam and then sloping the ion beam down through it. A form factor was then determined from the measured beam densities. Data were collected at a given center-of-mass energy  $E_{c.m.}$  until the required statistical precision was reached.  $E_{c.m.}$  was then changed a few percent to a new value by precisely scaling the magnetic field and the voltages on the electron gun, merger, and demerger before more data were taken at this new energy. This procedure was repeated several times to cover a given energy range. Beam profiles were measured again after data collection at several energies to check that the form factor had not deviated significantly during the scalings of the electron configuration.

### C. Adjustments to data

#### 1. Center-of-mass energy scale

The absolute energy scale of the measurements was determined by fitting the experimental data with a convolution of

two step functions at the spectroscopic thresholds for the  ${}^2P_{1/2}$  and  ${}^2P_{3/2}$  levels (i.e., at 6.656 eV and 6.685 eV, respectively), assuming a Gaussian energy distribution. The magnitudes of the step functions were statistically weighted. Results of the nonlinear least-squares fit demonstrated that, aside from our normally encountered contact potential of 2.0 V, no shift in the experimental center-of-mass energies was needed to achieve agreement with the spectroscopic thresholds. The energy spread full width at half maximum (FWHM) was determined to be 0.17 eV using this fitting procedure.

### 2. Below threshold spurious signal

Despite extreme care in preventing elastically scattered electrons from reaching the PSD and in reducing the individual backgrounds of the two beams, a persistent in-phase signal was measured below the  ${}^2P_{1/2}$  excitation threshold. This signal was likely due to the modulation of the background of one beam by the space charge of the other beam. This apparent background cross section, amounting to approximately 8% of the peak excitation cross section, was found to be independent of the center-of-mass energy, and was constant in time; consequently, it was subtracted from all the measured cross sections. Additional uncertainty for this subtraction procedure was included in the total experimental uncertainty, as discussed below.

### 3. Signal losses in the demerger

At center-of-mass energies sufficiently above the excitation threshold, the scattered electron velocity can exceed the ion velocity, so that an electron scattered at a large enough angle in the c.m. system may be moving backwards in the laboratory frame [6]. These electrons do not reach the PSD. For the energy range of the present experiment, backscattering should not contribute to signal loss. This was verified by trajectory modeling calculations using the SIMION [17] code. However, modeling did indicate that at the highest energy points, a small fraction of electrons was lost off the end of the PSD due to insufficient deflection by the demerger voltage applied. Higher demerger voltages could not be used in these cases without a large increase in the background count rates and an accompanying increase in spurious signal. The SIMION modeling was used to correct the measured cross sections, with corrections varying from  $\pm 4.7\%$  at 6.83 eV to  $\pm 8.3\%$  at 7.03 eV. No corrections were necessary for energies less than 6.83 eV.

### D. Uncertainties

The relative uncertainties of the measurements are a consequence of the statistical precision of the cross-section measurements, form-factor variations between individual points, and corrections predicted by the trajectory modeling. The relative uncertainties given represent a 90% confidence level (CL) for statistical precision. The total expanded uncertainties of the data also include the following systematic contributions, given at a level equivalent to 90% confidence for statistics: spatially delimiting the signal on the PSD ( $\pm 5\%$ ), detector efficiency ( $\pm 4\%$ ), absolute form factors

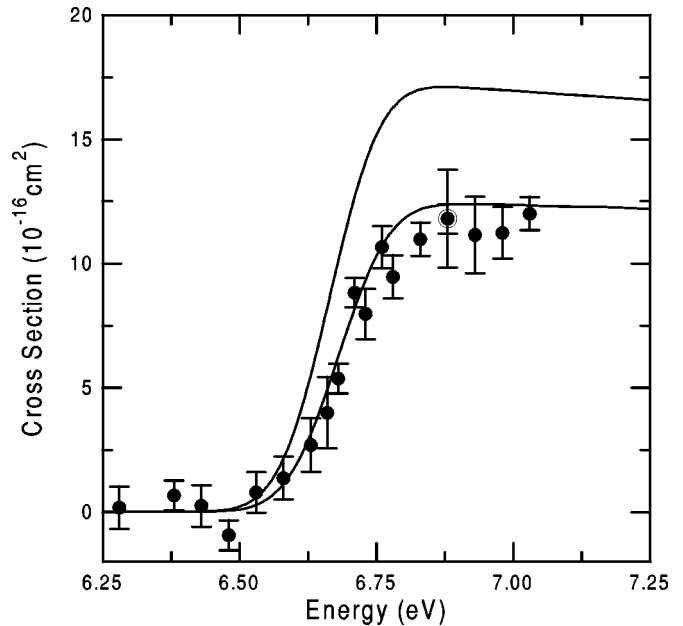


FIG. 2. Absolute cross sections for the excitation of  $\text{Al}^{2+} 3s^2S \rightarrow 3p^2P$  transition by electron impact as a function of center-of-mass energy. Solid circles are present results with error bars representing a 90% confidence level of relative uncertainties, with the exception of the point at 6.88 eV where the outer error bar represents the total expanded uncertainty. The solid curves are convolutions of theories with a 0.17 eV FWHM Gaussian: upper curve, UDW results of Ref. [10]; lower curve, CCV9 results of Ref. [11].

( $\pm 14\%$ ), electron and ion currents ( $\pm 1\%$  each), ion beam purity ( $\pm 2\%$ ), and subtraction of spurious below-threshold signal ( $\pm 3\%$ ). Added in quadrature, these contribute about  $\pm 16\%$  to the total expanded uncertainties. Systematic uncertainties associated with measurement of the electron and ion velocities and with the dead-time corrections are negligible.

## III. RESULTS

The measured electron-impact excitation cross sections for the  $3s^2S \rightarrow 3p^2P$  transition in  $\text{Al}^{2+}$  are shown as solid symbols in Fig. 2. The error bars represent relative uncertainties at a 90% confidence level. Also shown for the data point at 6.88 eV is the total expanded uncertainty of the measurement, indicated by the outer error bars on that point. Two calculations convoluted with a 0.17 eV Gaussian energy distribution are also shown in Fig. 2: the upper curve represents the unitarized distorted wave predictions of Merts *et al.* [10], and the lower curve represents the nine-state close-coupling predictions of Mitroy and Norcross [11]. It is clear from Fig. 2 that the present experimental data agree better with the more sophisticated nine-state close coupling calculations of Mitroy and Norcross (lower solid curve). The measurements of Dunn *et al.* [9] are not shown in Fig. 2 since the much broader energy resolution of the previous experiment results in only two of their data points lying in the energy range of Fig. 2. The present results yield an excitation step (at threshold) of  $(11.4 \pm 1.9) \times 10^{-16} \text{ cm}^2$ , whereas the results of Dunn *et al.* yield  $(16.0 \pm 3.0) \times 10^{-16} \text{ cm}^2$ . Hence, the two measurements barely agree within the total expanded uncertainties (90% CL).

#### IV. CONCLUSIONS

In summary, absolute cross sections for electron-impact excitation of the  $3s\ ^2S \rightarrow 3p\ ^2P$  transition in  $\text{Al}^{2+}$  have been measured using the MEIBEL technique. When the energy resolutions and the total experimental uncertainties at a 90% CL are included, the present results barely overlap with the measurements of Dunn *et al.* [9] made with a crossed-beam fluorescence technique. Our measurements favor the close-coupling calculations (CCV9) of Mitroy and Norcross [11] over the unitarized distorted-wave (UDW) calculations of Merts *et al.* [10]. While one might anticipate such agreement with the more sophisticated theoretical approach, this is not always the case. In the case of the first allowed transition in  $\text{C}^{3+}$ , for example, energy-loss measurements [18,19] fa-

vored Coulomb-Born predictions while fluorescence measurements of Savin *et al.* [20] agreed better with the close-coupling results. Continued experimental investigations of electron-impact excitation are needed to provide further guidance to theoretical efforts.

#### ACKNOWLEDGMENTS

This work was supported in part by the Office of Fusion Energy Sciences of the U.S. Department of Energy under Contract No. DE-AC05-00OR22725 with UT-Battelle, LLC, and Contract No. DE-A102-95ER54293 with the National Institute of Standards and Technology. Y.S.C. was supported by the Korean Science and Engineering Foundation Grant No. R01-2001-00020.

- 
- [1] D.R. Flower and H. Nussbaumer, *Astron. Astrophys.* **42**, 265 (1975).
- [2] F. P. Keenan, in *UV and X-ray Spectroscopy of Laboratory and Astrophysical Plasmas*, edited by E.H. Silver and S.M. Kahn, (Cambridge University Press, Cambridge, 1993), p. 44.
- [3] S.J. Smith, A. Chutjian, J. Mitroy, S.S. Tayal, R.J.W. Henry, K.-F. Man, R.J. Mawhorter, and I.D. Williams, *Phys. Rev. A* **48**, 292 (1993).
- [4] E.K. Wählin, J.S. Thompson, G.H. Dunn, R.A. Phaneuf, D.C. Gregory, and A.C.H. Smith, *Phys. Rev. Lett.* **66**, 157 (1991).
- [5] N. Djurić, M.E. Bannister, A.M. Derkatch, D.C. Griffin, H.F. Krause, D.B. Popović, A.C.H. Smith, B. Wallbank, and G.H. Dunn, *Phys. Rev. A* **65**, 052711 (2002).
- [6] X.Q. Guo, E.W. Bell, J.S. Thompson, G.H. Dunn, M.E. Bannister, R.A. Phaneuf, and A.C.H. Smith, *Phys. Rev. A* **47**, R9 (1993).
- [7] R.K. Janev, in *Atomic and Plasma-Material Interaction Processes in Controlled Thermonuclear Fusion*, edited by R.K. Janev and H.W. Drawin (Elsevier, Amsterdam, 1993), p. 27.
- [8] J.D.F. Bartoe, G.E. Brueckner, J.D. Purcell, and R. Tousey, *Appl. Opt.* **16**, 879 (1977).
- [9] G.H. Dunn, D.S. Belić, C. Cisneros, D.H. Crandall, R.A. Falk, and D.C. Gregory, *Phys. Rev. A* **66**, 032706 (2002).
- [10] A.L. Merts, J.B. Mann, W.D. Robb, and N.H. Magee, Jr., Los Alamos Laboratory Informal Report No. LA-8267-MS, 1980.
- [11] J. Mitroy and D.W. Norcross, *Phys. Rev. A* **39**, 537 (1989).
- [12] E.W. Bell, X.Q. Guo, K. Rinn, D.R. Swenson, J.S. Thompson, G.H. Dunn, M.E. Bannister, D.C. Gregory, R.A. Phaneuf, A.C.H. Smith, A. Müller, C.A. Timmer, E.K. Wählin, B.D. DePaola, and D.S. Belić, *Phys. Rev. A* **49**, 4585 (1994).
- [13] F.W. Meyer, in *Trapping Highly Charged Ions: Fundamentals and Applications*, edited by J. Gillaspay (Nova Science, Huntington, NY, 2001), p. 117.
- [14] D. Hitz, G. Melin, M. Pontonnier, and T.K. Nguyen, Kernfysisch Versneller Instituut Report No. 996, 1993 (unpublished).
- [15] J.L. Forand, C.A. Timmer, E.K. Wählin, B.D. DePaola, G.H. Dunn, D. Swenson, and K. Rinn, *Rev. Sci. Instrum.* **61**, 3372 (1990).
- [16] CIDTEC model CID 2250D solid-state video camera. This information is provided for technical completeness and not as a product or company endorsement.
- [17] D.A. Dahl, SIMION 3D, Version 6. 0, Idaho National Engineering Laboratory Report No. INEL-95/0403, 1995.
- [18] M.E. Bannister, Y.-S. Chung, N. Djurić, B. Wallbank, O. Voitke, S. Zhou, G.H. Dunn, and A.C.H. Smith, *Phys. Rev. A* **57**, 278 (1998).
- [19] J.B. Greenwood, S.J. Smith, A. Chutjian, and E. Pollack, *Phys. Rev. A* **59**, 1348 (1999).
- [20] D.W. Savin, L.D. Gardner, D.B. Reisenfeld, A.R. Young, and J.L. Kohl, *Phys. Rev. A* **51**, 2162 (1995).